International Journal of Control, Automation and Systems 17(5) (2019) 1117-1130
http://dx.doi.org/10.1007/s12555-017-0717-7
ISSN:1598-6446 eISSN:2005-4092
http://www.springer.com/12555

Distributed Fixed-time Attitude Synchronization Control for Multiple Rigid Spacecraft

Wei-Shun Sui*, Guang-Ren Duan, Ming-Zhe Hou, and Mao-Rui Zhang

Abstract: This paper investigates the distributed fixed-time attitude synchronization control problem for multiple rigid spacecraft system with external disturbances. Based on sliding-mode estimators, the authors remove the requirement of neighbours' input control information. Using the fixed-time-based terminal sliding mode, the distributed adaptive control laws are developed to guarantee the attitude tracking errors converge to the regions in fixed time independent of initial conditions, and adaptive laws are employed to deal with external disturbances. Finally, numerical simulations are presented to illustrate the performance of the proposed controllers.

Keywords: Attitude synchronization, distributed adaptive control, fixed-time-based terminal sliding mode, sliding-mode estimator.

1. INTRODUCTION

With the development of aerospace technology, various spacecraft are becoming more and more complex and costly. To replace a large and costly spacecraft with a group of smaller, less-expensive, and cooperative spacecraft, the concept of spacecraft formation flying (SFF) is presented. As part of SFF, distributed attitude synchronization control of multi-spacecraft becomes a new technology for many missions such as Terrestrial Planet Finder [1], synthetic aperture imaging [2], and in-orbit servicing and maintenance of spacecraft. Due to the above advantages, research on distributed attitude synchronization has received considerable attention over the last decade.

The attitude synchronization control of rotating rigid bodies is studied in [3], where the leader tracks a predefined orientation and the followers' orientations track the leader. In [4, 5], the synchronization attitude control problem for a group of spacecraft without velocity measurements is studied. Abdessameud [6] considered the attitude synchronization control problem with communication delays, while Zou [7] considered this problem with input saturation. However, all these aforementioned literatures only gain asymptotic convergence, and can't provide finite-time control which is more significant in practical application. In the SFF attitude synchronization control, the finite-time control can provide faster convergence rate and better disturbance rejection properties, therefore, it is highly desirable to develop a distributed finite-time attitude synchronization control approach.

It is well known that terminal sliding mode control (TSMC) is an effective finite-time control scheme, especially for systems with uncertainties and disturbances [8, 9]. Based on terminal sliding mode, two finite-time controllers are developed to drive a rigid spacecraft to track a desired attitude in finite time in the presence of external disturbances in [10]. Based on the behaviour approach, a class of continuous sliding mode control schemes were developed in [11], which achieved finite-time convergence of spacecraft attitude under arbitrary communication topologies. For spacecraft formation problem under uncertain time-varying topologies, [12] proposed a class of decentralized attitude control schemes by using terminal sliding mode control. However, the input control signal of each follower need the input control information of the neighbours in most literatures, and the controllers are indeed not a distributed, but a decentralised one. In this situation, the communication flow among neighbors increases and an algebraic loop yields. In addition, in order to overcome slow convergence problem existing in TSM, the fast terminal sliding mode (FTSM) is proposed by Yu and Man [13]. Zou [14] proposed a distributed attitude coordination control scheme using FTSM for a group of spacecraft in the presence of external disturbances, which achieved finite-time stability of the overall closed-loop system. Furthermore, in order to eliminate the singular-

Manuscript received November 15, 2017; revised March 15, 2018 and October 7, 2018; accepted January 13, 2019. Recommended by Associate Editor Chang Kyung Ryoo under the direction of Editor Duk-Sun Shim. This paper was supported by the Major Program of National Natural Science Foundation of China under Grant Numbers 61690210 and 61690212; the National Natural Science Foundation of China 61333003; the Self-Planned Task (NO.SKLRS201716A) of State Key Laboratory of Robotics and System (HIT).

Wei-Shun Sui, Guang-Ren Duan, Ming-Zhe Hou, and Mao-Rui Zhang are with Center for Control Theory and Guidance Technology, Harbin Institute of Technology, 2 Yi Kuang Street, Nan Gang District, Harbin 150001, China (e-mails: suiweishunhit@163.com, g.r.duan@hit.edu.cn, hithyt@hit.edu.cn, zhangmaorui@hit.edu.cn).
* Corresponding author.

ity problem existing in FTSM, a novel concept of nonsingular fast TSM (NFTSM) is proposed in [15]. Based on NFTSM, a decentralized adaptive control scheme is developed under inertia uncertainties and external disturbances with unknown bounds in [17], which can guarantee the attitude tracking errors converge to the regions containing the origin in finite time. Although there are fruitful results on finite-time approaches for attitude synchronization control of multi-spacecraft system, the settling time of all above control approaches are dependent of initial conditions, implying that the convergence time will be long if initial state of the system is far away from the desired state. However, the time indexes are predefined in many practical engineering applications, and the corresponding required time could not be satisfied if the settling time are dependent of initial conditions.

To address above mentioned problems, the concept of fixed-time convergence was proposed in [18], which confined the settling time independent of initial conditions, but only related to design parameters. Inspired by the above discussions, in this paper, we investigate the fixed-time attitude synchronization control problem for SFF in the presence of external disturbances with unknown bounds. We construct a sliding-mode estimator and based on which, a distributed fixed-time controller without using the input control information of the neighbours is proposed. The main contributions of this paper are stated as follows:

1) A fixed-time-based sliding manifold based on attitude state errors is proposed for the attitude synchronization control of multiple rigid spacecraft. Comparing with TSM employed in [14] and [17], the settling time of the fixed-time-based sliding manifold is independent of initial conditions. By choosing suitable parameters, the settling time can be designed to satisfy the requirements in practical application.

2) Based on the concept of fixed-time convergence, a novel sliding mode estimator is constructed. In contrast to [19], which provides finite-time estimate of the leader's attitude state and angular velocity, we propose the fixed-time sliding mode estimator which can provide the accurate estimate of the leader's state. It is clear that the fixed-time sliding mode estimator is more effective in practical application.

3) By combining the sliding-mode estimator and adaptive control, the distributed control laws employing fixed-time-based sliding manifold are proposed for multiple rigid spacecraft with external disturbances. The proposed controller can achieve the attitude synchronization control of multiple rigid spacecraft in fixed-time. In contrast to [17], using the sliding-mode estimator, we remove the requirement that all the follower spacecraft need the information of the leader and the input torques of the neighbours, then avoiding the algebraic loop problem. To the best of our knowledge, this paper is the first to deal with the distributed attitude synchronization control problem in fixed-time without using the input information of the neighbours.

The remaining of this paper is organized as follows: In Section 2, the dynamics of rigid spacecraft attitude, algebraic graph theory and some lemmas adopting in main results are briefly described. The main result is presented in Section 3. Simulation results are shown in Section 4 and the conclusion follows in Section 5.

The following notations will be used throughout the paper. $\mathbb{R}$ stands for the set of real numbers. $\mathbb{R}_+$ represents the set of positive real numbers. $\mathbb{R}^n$ is the n-dimensional real vector space. $\mathbb{R}^{n\times n}$ denotes the set of $n\times n$ matrices. $\lambda_{\min}(A)$ represents the minimum eigenvalue of matrix A. $\|\cdot\|$ is the standard Euclidean vector norm. Let $\mathrm{sig}^a x \triangleq \mathrm{sign}(x)\,|x|^a$, where $a>0$, $x\in\mathbb{R}$, $\mathrm{sign}(x)$ is sign function, and $|\cdot|$ refers to the absolute value. Furthermore, we define $\mathrm{sig}^a z = [\mathrm{sig}^a z_1,\ldots,\mathrm{sig}^a z_n]^{\mathrm{T}}$ and $\mathrm{sign}(z) = [\mathrm{sign}(z_1),\ldots,\mathrm{sign}(z_n)]^{\mathrm{T}}$, where $z\in\mathbb{R}^n$ and $z=[z_1,\ldots,z_n]^{\mathrm{T}}$.

2. BACKGROUND AND PRELIMINARIES

2.1. Dynamics of rigid spacecraft attitude

We consider a multiple rigid spacecraft system consisting of n followers indexed by 1 to n, and one leader indexed by 0. The attitude of every follower is represented by Modified Rodriguez Parameters (MRPs) given by [20]

$$q_i(t) = \rho_i \tan\left(\frac{\phi_i(t)}{4}\right),\quad \phi_i\in[0,2\pi)\ \mathrm{rad}, \tag{1}$$

where $q_i\in\mathbb{R}^3$ is the MRPs denoting the rotation from the body frame of the ith rigid body to the inertial frame, ρ_i and ϕ_i denote the Eular eigenaxis and eigenangle of the attitude of the ith rigid body. As shown in [21], since the shadow set of MRPs $q_i^S = -\frac{q_i}{\|q_i\|^2}$ represents the same attitude as q_i, we can always keep the magnitude of the MRPs vector from exceeding unity by switching to the shadow MRPs. From [17], we have $\|q_i\|\le 1$ by switching between MRPs q_i and its shadow counterpart q_i^S. Attitude kinematics and dynamics of the ith spacecraft in the formation are given by [17]

$$J_i\dot{\omega}_i = -\omega_i^{\times} J_i\omega_i + u_i + d_i, \tag{2}$$

$$\dot{q}_i = T_i(q_i)\omega_i,\quad i=1,\ldots,n, \tag{3}$$

where $J_i\in\mathbb{R}^{3\times 3}$ is the symmetric inertia matrix of the ith spacecraft, $\omega_i\in\mathbb{R}^3$ is the angular velocity of the ith spacecraft with respect to the inertial frame, $u_i\in\mathbb{R}^3$ is the control torque in the formation, $d_i\in\mathbb{R}^3$ is the unknown external disturbance torque. $\omega_i^{\times}$ is the skew-symmetric matrix with the form

$$\omega_i^{\times} = \begin{bmatrix} 0 & -\omega_{i3} & \omega_{i2} \\ \omega_{i3} & 0 & -\omega_{i1} \\ -\omega_{i2} & \omega_{i1} & 0 \end{bmatrix}. \tag{4}$$

The Jacobian matrix $T_i(q_i) \in \mathbb{R}^{3\times3}$ is given by [21]

$$T_i(q_i) = \frac{1}{2}\left(\frac{1-q_i^{\mathrm{T}}q_i}{2}I_3 + q_i^{\times} + q_i q_i^{\mathrm{T}}\right), \tag{5}$$

where $I_3 \in \mathbb{R}^{3\times3}$ denotes the identity matrix.

The attitude of the leader is the time-varying reference attitude q_d for the whole group. In order to facilitate the control development, the following assumptions with respect to the reference trajectory q_d and external disturbances are given.

Assumption 1: The reference trajectory q_d is constructed to avoid the kinematic singular associate with the modified Rodrigues parameters.

Assumption 2: The reference trajectory q_d and its first two derivatives $\dot{q}_d$ and $\ddot{q}_d$ are assumed to be bounded.

Assumption 3: There exists an unknown constant d_0 such that the external disturbance d_i satisfies

$$\|d_i(t)\| \le d_0. \tag{6}$$

In addition, we assume the inertia matrix J_i of each spacecraft keep constant and can be measured precisely, thus the norm of the inertia matrix $\|J_i\|$ is a known positive constant.

2.2. Attitude dynamics in Lagrange expression

We first denote $T_i(q_i)^{-1} = P_i(q_i)$, then the ith spacecraft attitude dynamics (2) and kinematics (3) can be transformed into the Lagrange expression [22]

$$M_i(q_i)\ddot{q}_i + C_i(q_i,\dot{q}_i)\dot{q}_i = P_i^{\mathrm{T}}u_i + P_i^{\mathrm{T}}d_i, \tag{7}$$

where $M_i(q_i) = P_i^{\mathrm{T}}J_iP_i$, $C_i(q_i,\dot{q}_i) = -M_i\dot{T}_iP_i - P_i^{\mathrm{T}}(J_iP_i\dot{q}_i)^{\times}P_i$. By appropriate procedures, we can have

$$\ddot{q}_i = h_i + \bar{u}_i + g_i, \tag{8}$$

where $h_i = \left[\dot{T}_iP_i + T_iJ_i^{-1}(J_iP_i\dot{q}_i)^{\times}P_i\right]\dot{q}_i$, $\bar{u}_i = T_iJ_i^{-1}u_i$, and $g_i = T_iJ_i^{-1}d_i$.

Note that the approaches developed in this paper are based on Lagrange expression (7), therefore the control scheme in this paper can be applied to other mechanical systems as long as those representations can be transformed in a Lagrange form, such as the rigid-link robot manipulator.

2.3. Algebraic graph theory

Graphs can be used to represent the topology of the information flow between spacecraft in the formation. Let $G = (V,\varepsilon,A)$ be a undirected weighted graph, in which $V = \{v_1,\ldots,v_N\}$ is a nonempty set of spacecraft nodes and $\varepsilon = V\times V$ is a set of edges. An edge of undirected graph G is defined as $e_{ij} = (v_i,v_j)$ denoting that the node v_j can receive the state of node v_i and vice versa, i.e., $e_{ij}\in\varepsilon \Leftrightarrow e_{ji}\in\varepsilon$. The adjacency matrix $A = [a_{ij}] \in \mathbb{R}^{N\times N}$ of graph G is defined such that adjacency elements a_{ij} satisfy $a_{ij} = 1$ if $e_{ji}\in\varepsilon$ and $e_{ji} = 0$ otherwise. Morever, we exclude the self-loop case, i.e., $a_{ii} = 0$ for all $i\in\{1,2,\ldots,n\}$. Let $N_i = \{v_j\in V : (v_i,v_j)\in\varepsilon\}$ be the neighbours set of spacecraft v_i. For any two nodes i and j, if there exists a path between them, then graph G is called a connected graph. In this paper, the graph G is undirected connected graph.

The in-degree diagonal matrix is defined as $D = \mathrm{diag}(d_1,\ldots,d_n)$, whose diagonal elements are given by $d_i = \sum_{j\in N_i} a_{ij}$.Then the Laplacian matrix L of the weighted graph G is defined by $L = D - A$. When the multiple rigid spacecraft system consists of a leader, we use $\bar{G}$ to represent the topology in this case. Leader adjacency matrix is defined as $B = \mathrm{diag}\{b_1,b_2,\ldots,b_n\}$, where $b_i = 1$ if spacecraft v_i is connected to the leader and $b_i = 0$ otherwise. We also denote $H = L + B$.

2.4. Definitions and Lemmas

Consider the following system:

$$\dot{z} = g(t,z),\ \ z(0) = z_0, \tag{9}$$

where $z\in\mathbb{R}^n$ and $g:\mathbb{R}_+\times\mathbb{R}^n \longrightarrow \mathbb{R}^n$ is a nonlinear function which may be discontinuous, the solutions of (9) are understood in the sense of Filippov [23]. Assume the origin is an equilibrium point of (9).

Definition 1 [18]**:** The origin of (9) is said to be globally finite-time stable if it is globally asymptotically stable and any solution $z(t,z_0)$ of (9) reaches the equilibria at some finite time moment, i.e., $z(t,z_0) = 0$, $\forall t \ge T(z_0)$, where $T:\mathbb{R}^n \longrightarrow \mathbb{R}_+\cup\{0\}$ is the settling-time function.

Definition 2 [18]**:** The origin of (9) is said to be fixed-time stable if it is globally finite-time stable and the settling-time function $T(z_0)$ is bounded, i.e., $\exists T_{\max} > 0$: $T(z_0) \le T_{\max}$, $\forall z_0\in\mathbb{R}^n$.

Before giving the main result, some lemmas are introduced which will contribute much to proof of stability.

Lemma 1 [25]**:** Let $\xi_1,\xi_2,\ldots,\xi_N \ge 0$. Then

$$\sum_{i=1}^{N}\xi_i^p \ge \left(\sum_{i=1}^{N}\xi_i\right)^p,\ \text{if } 0<p\le 1, \tag{10}$$

$$\sum_{i=1}^{N}\xi_i^p \ge N^{1-p}\left(\sum_{i=1}^{N}\xi_i\right)^p,\ \text{if } 1<p<\infty. \tag{11}$$

Denote $D^+\varphi(t)$ by the upper right-hand derivative of a function $\varphi(t)$, $D^+\varphi(t) = \lim\limits_{h\to0+}\sup\frac{\varphi(t+h)-\varphi(t)}{h}$.

Lemma 2 [27]**:** Consider the system (9), if there exists a continuous radially unbounded function $V:\mathbb{R}^n \longrightarrow \mathbb{R}_+\cup\{0\}$ such that

1) $V(z) = 0 \Leftrightarrow z = 0$;

2) any solution $z(t)$ of (9) satisfies the inequality $D^*V(z(t)) \leq -(\alpha V^p(z(t)) + \beta V^q(z(t)))^k$ for some $\alpha, \beta, p, q, k > 0 : pk < 1, qk > 1$,
then the origin is globally fixed-time stable for system (9) and the following estimate holds:

$$T(z_0) \leq \frac{1}{\alpha^k(1-pk)} + \frac{1}{\beta^k(qk-1)} \quad \forall z_0 \in \mathbb{R}^n \tag{12}$$

Lemma 3 [28]**:** For any positive scalar $\nu > \frac{1}{2}, \tilde{a}\hat{a} \leq \frac{-(2\nu-1)}{2\nu}\tilde{a}^2 + \frac{\nu}{2}a^2$ with $\tilde{a} = a - \hat{a}$.

Lemma 4 [14]**:** If $\bar{G}$ is connected, then the matrix H associated with $\bar{G}$ is symmetric and positive definite.

2.5. Problem formulation

The attitude state error of an individual spacecraft with respect to the reference attitude state is denoted as

$$e_{1i} = q_i - q_d, \tag{13}$$
$$e_{2i} = \dot{q}_i - \dot{q}_d, \quad i = 1, \ldots, n. \tag{14}$$

The dynamic equations for the attitude state errors of the ith spacecraft in the formation can be expressed as

$$\dot{e}_{1i} = e_{2i}, \tag{15}$$
$$\dot{e}_{2i} = h_i - \ddot{q}_d + \bar{u}_i + g_i, \quad i = 1, \ldots, n. \tag{16}$$

The goal of this paper is to design distributed attitude control law u_i for the n rigid spacecraft such that all spacecraft attitudes reach synchronization, meanwhile track the reference attitude in fixed time.

3. MAIN RESULT

3.1. Fixed-time-based sliding mode surface design

In many researches, the terminal sliding mode (TSM) and the nonsingular TSM (NTSM) are commonly used for rigid spacecraft attitude control. In order to improve convergence rate, fast terminal sliding mode (FTSM) and nonsingular FTSM (NFTSM) are adopted by [14] and [17] respectively. The expressions can be defined by the following differential equations:

$$\text{FTSM: } s = \dot{x} + \sigma_1 x + \sigma_2 x^{p/q}, \tag{17}$$
$$\text{NFTSM: } s = x + \sigma_1 \text{sig}^{\gamma_1} x + \sigma_2 \text{sig}^{\gamma_2} \dot{x}, \tag{18}$$

where $\text{sig}^{\gamma_1} x = \text{sign}(x)|x|^{\gamma_1}$, $\text{sig}^{\gamma_2}\dot{x} = \text{sign}(\dot{x})|\dot{x}|^{\gamma_2}$, and $\text{sign}(x)$ is defined as

$$\text{sign}(x) = \begin{cases} 1, & x > 0, \\ 0, & x = 0, \\ -1, & x < 0, \end{cases}$$

besides, σ_1 and σ_2 are positive constants respectively, the positive odd integers p, q are chosen such that $\frac{1}{2} < p/q < 1$, and $1 < \gamma_2 < 2$, $\gamma_2 < \gamma_1$.

Remark 1: As shown in [16], since p, q are positive odd integers, FTSM (17) can be rewritten as $s = \dot{x} + \sigma_1 x + \sigma_2 \text{sig}^{p/q} x$. It is found that if the sliding manifold (17) $s = 0$ is reached, $x = 0$ will be reached in a finite time determined by

$$T_f = \frac{q}{\sigma_1(q-p)} \ln \frac{\sigma_1 x(0)^{\frac{q-p}{q}} + \sigma_2}{\sigma_2}. \tag{19}$$

Furthermore, the time derivative of the sliding manifold s defined by (17) is given by

$$\dot{s} = \ddot{x} + \sigma_1 \dot{x} + \frac{p\sigma_2}{q} x^{p/q-1} \dot{x}. \tag{20}$$

Unfortunately, due to $p/q - 1 < 0$, the singularity will occur if $x = 0$ and $\dot{x} \neq 0$. In order to overcome the drawback, NFTSM (18) is put forward. And the time derivative of the sliding manifold s defined by (18) is given by

$$\dot{s} = \dot{x} + \sigma_1 \gamma_1 |x|^{\gamma_1 - 1} \dot{x} + \sigma_2 \gamma_2 |\dot{x}|^{\gamma_2 - 1} \ddot{x}. \tag{21}$$

It is found that singularity dose not occur in this situation since $1 < \gamma_2 < \gamma_1$. For any given initial state $x(0)$ on NFTSM surface, the system state converges to $x = 0$ in finite time [17]

$$T_n = \frac{\gamma_2 |x(0)|^{1-\frac{1}{\gamma_2}}}{\sigma_1(\gamma_2 - 1)} F\left(\frac{1}{\gamma_2}, \frac{\gamma_2 - 1}{(\gamma_1 - 1)\gamma_2}; 1 + \frac{\gamma_2 - 1}{(\gamma_1 - 1)\gamma_2}; -\sigma_1 |x(0)|^{\gamma_1 - 1}\right), \tag{22}$$

where $F(\cdot)$ denotes Gauss' Hypergeometric function (see [29] for further details). Usually, the exact form of $F(\cdot)$ varies with the involved parameters. For example, $F(-n, b; b; -z) = (1+z)^n$; $F(1, 1; 2; -z) = \frac{\ln(1+z)}{z}$.

Obviously, the convergence time of above two sliding mode surfaces are dependent of initial state $x(0)$, implying that the convergence time will be long if initial state $x(0)$ is far away from the equilibrium point $x = 0$. In this situation, the required settling time could not be satisfied in practical application. In the design of the control system, we expect to obtain the fixed upper bound of the settling time. Thus, the fixed-time convergence concept is proposed by Polyakov [18].

Inspired by the work of [18,30], a fixed-time-based sliding manifold is proposed as

$$s = \text{sig}^{\frac{1}{k_1}} \dot{x} + \sigma_3 \text{sig}^{p_1} x + \sigma_4 \text{sig}^{g_1} x, \tag{23}$$

where $\sigma_3 > 0$, $\sigma_4 > 0$, $\frac{1}{2} < k_1 < 1$, $1 < p_1 < g_1$, $p_1 k_1 < 1$, $g_1 k_1 > 1$.

Remark 2: It can be noted that sliding manifold (23) is a transformation expression of NTSM in [30]. The advantage of (23) is that the range of the power p_1, g_1, k_1

is larger than that of the power m_i, n_i, $i = 1, 2, 3$ in [30], which is not restricted to positive odd integers. The time derivative of (23) is given by

$$\dot{s} = \frac{1}{k_1} |\dot{x}|^{\frac{1}{k_1}-1} \ddot{x} + \sigma_3 p_1 |x|^{p_1-1} \dot{x} + \sigma_4 g_1 |x|^{g_1-1} \dot{x}. \quad (24)$$

Due to $1 < \frac{1}{k_1}$, $1 < p_1 < g_1$, the singularity will not occur, and the fixed-time-based sliding mode is nonsingular. By a similar analysis in [30], we conclude that any given initial state can converge to $x = 0$ in fixed time, with a settling time

$$T_{ft} = \frac{1}{\sigma_3^{k_1}(1 - p_1 k_1)} + \frac{1}{\sigma_4^{k_1}(g_1 k_1 - 1)}. \quad (25)$$

It is obvious that T_{ft} is independent of initial state $x(0)$, and only with regard to parameters which can be designed in advance. Therefore the upper bound of the settling time could be estimated without requiring knowledge of the initial conditions, and the settling time could be shorter than that of FTSM (17) and NFTSM (18) when initial state is far away from $x = 0$.

3.2. Construction of the fixed-time sliding-mode estimator

In most literatures, all the followers need the information of the leader and the input control torques of neighbours, which increases the communication flow among neighbor spacecraft in the formation and the cost of SFF task, meanwhile yields an algebraic loop problem existing in the controller presented in [31]. In order to solve these problems, two distributed fixed-time sliding-mode estimators are introduced in the following discussion, which are used to obtain the accurate estimates of q_d and $\dot{q}_d$, respectively. The expressions are given as

$$\begin{aligned}\dot{\hat{q}}_i = &-\beta_1^{-\frac{1}{a_2}} \mathrm{sig}^{\frac{1}{a_2}} \left[\sum_{j\in N_i} a_{ij}(\hat{q}_i - \hat{q}_j) + b_i(\hat{q}_i - q_d) \right. \\ &\left. + \alpha_1 \mathrm{sig}^{a_1} \left(\sum_{j\in N_i} a_{ij}(\hat{q}_i - \hat{q}_j) + b_i(\hat{q}_i - q_d) \right) \right] \\ &- \lambda_1 \mathrm{sign} \left[\sum_{j\in N_i} a_{ij}(\hat{q}_i - \hat{q}_j) + b_i(\hat{q}_i - q_d) \right], \quad (26)\end{aligned}$$

$$\begin{aligned}\dot{\hat{v}}_i = &-\beta_1^{-\frac{1}{a_2}} \mathrm{sig}^{\frac{1}{a_2}} \left[\sum_{j\in N_i} a_{ij}(\hat{v}_i - \hat{v}_j) + b_i(\hat{v}_i - \dot{q}_d) \right. \\ &\left. + \alpha_1 \mathrm{sig}^{a_1} \left(\sum_{j\in N_i} a_{ij}(\hat{v}_i - \hat{v}_j) + b_i(\hat{v}_i - \dot{q}_d) \right) \right] \\ &- \lambda_2 \mathrm{sign} \left[\sum_{j\in N_i} a_{ij}(\hat{v}_i - \hat{v}_j) + b_i(\hat{v}_i - \dot{q}_d) \right], \quad (27)\end{aligned}$$

where $\hat{q}_i$ and $\hat{v}_i$ are respectively the estimate of q_d and $\dot{q}_d$, $\alpha_1 > 0$, $\beta_1 > 0$, $1 < a_2 < 2$, $a_1 > a_2$, λ_1 and λ_2 are positive constants.

Two proofs of two estimators are similar, so we choose to proof the first estimator.

Proposition 1: Consider a multiple spacecraft system modeled as (2)-(3) under Assumptions 1 and 2, and a distributed sliding-mode estimator is designed as (26) for the ith follower. If $\lambda_1 > \vartheta_1 = \sup|\dot{q}_{dm}|$, $m = 1, 2, 3$, then $\hat{q}_i - q_d$ converges to zero in fixed time.

Proof: Let $e_{qi} = \hat{q}_i - q_d$, $e_q = [e_{q1}^{\mathrm{T}}, \ldots, e_{qn}^{\mathrm{T}}]^{\mathrm{T}}$, then we have

$$\begin{aligned}\dot{e}_{qi} = &-\beta_1^{-\frac{1}{a_2}} \mathrm{sig}^{\frac{1}{a_2}} \left[\sum_{j\in N_i} a_{ij}(e_{qi} - e_{qj}) + b_i e_{qi} \right. \\ &\left. + \alpha_1 \mathrm{sig}^{a_1} \left(\sum_{j\in N_i} a_{ij}(e_{qi} - e_{qj}) + b_i e_{qi} \right) \right] \\ &- \lambda_1 \mathrm{sign} \left[\sum_{j\in N_i} a_{ij}(e_{qi} - e_{qj}) + b_i e_{qi} \right] - \dot{q}_d, \quad (28)\end{aligned}$$

and the vector form can be written as

$$\begin{aligned}\dot{e}_q = &-\beta_1^{-\frac{1}{a_2}} \mathrm{sig}^{\frac{1}{a_2}} [(H \otimes I_3)e_q + \alpha_1 \mathrm{sig}^{a_1}((H \otimes I_3)e_q)] \\ &- \lambda_1 \mathrm{sign}((H \otimes I_3)e_q) - 1_N \otimes \dot{q}_d, \quad (29)\end{aligned}$$

where $\otimes$ denotes the Kronecker product and $1_N = [1, \ldots, 1]^{\mathrm{T}}$.

Based on Lemma 4 and the property of Kronecker product, we obtain that $H \otimes I_3$ is positive definite. Then we define a Lyapunov function as $V_q = \frac{1}{2} e_q^{\mathrm{T}}(H \otimes I_3)e_q$, and let $\rho = (H \otimes I_3)e_q$, i.e., $\rho = [\rho_{11}, \rho_{12}, \ldots, \rho_{n2}, \rho_{n3}]^{\mathrm{T}}$, then taking the time derivative of V_q, we obtain

$$\begin{aligned}\dot{V}_q = &-\beta_1^{-\frac{1}{a_2}} \sum_{i=1}^{n}\sum_{m=1}^{3} \rho_{im} \mathrm{sign}(\rho_{im} + \alpha_1 \mathrm{sign}(\rho_{im})) \\ &\times ||\rho_{im}| \mathrm{sign}(\rho_{im}) + \alpha_1 \mathrm{sign}(\rho_{im}) |\rho_{im}|^{a_1}|^{\frac{1}{a_2}} \\ &- \lambda_1 \sum_{i=1}^{n}\sum_{m=1}^{3} |\rho_{im}| - \sum_{i=1}^{n}\sum_{m=1}^{3} \rho_{im}\dot{q}_{dm} \\ \le &-\beta_1^{-\frac{1}{a_2}} \sum_{i=1}^{n}\sum_{m=1}^{3} |\rho_{im}^{a_2}|^{\frac{1}{a_2}} (|\rho_{im}| + \alpha_1 |\rho_{im}|^{a_1})^{\frac{1}{a_2}} \\ &- (\lambda_1 - \vartheta_1) \sum_{i=1}^{n}\sum_{m=1}^{3} |\rho_{im}| \\ \le &-\beta_1^{-\frac{1}{a_2}} \left(\sum_{i=1}^{n}\sum_{m=1}^{3} (\rho_{im}^2)^{\frac{a_2+1}{2}} + \sum_{i=1}^{n}\sum_{m=1}^{3} \alpha_1 (\rho_{im}^2)^{\frac{a_1+a_2}{2}} \right)^{\frac{1}{a_2}} \\ \le &-\beta_1^{-\frac{1}{a_2}} [(3N)^{\frac{1-a_2}{2}} \left(\sum_{i=1}^{n}\sum_{m=1}^{3} \rho_{im}^2 \right)^{\frac{a_2+1}{2}} \\ &+ \alpha_1 (3N)^{\frac{2-a_1-a_2}{2}} \left(\sum_{i=1}^{n}\sum_{m=1}^{3} \rho_{im}^2 \right)^{\frac{a_1+a_2}{2}}]^{\frac{1}{a_2}} \\ \le &-\left(\frac{\varsigma_1}{\beta_1} V_q^{\frac{a_2+1}{2}} + \frac{\alpha_1}{\beta_1} \varsigma_2 V_q^{\frac{a_1+a_2}{2}} \right)^{\frac{1}{a_2}}, \quad (30)\end{aligned}$$

where $\varsigma_1 = (3N)^{\frac{1-a_2}{2}}(2\lambda_{\min}(H))^{\frac{a_2+1}{2}}$, and $\varsigma_2 = (3N)^{\frac{2-a_1-a_2}{2}} \times (2\lambda_{\min}(H))^{\frac{a_1+a_2}{2}}$, and Lemma 1 has been used in above inequality. Due to $\frac{a_2+1}{2}\cdot\frac{1}{a_2} < 1$, $\frac{a_1+a_2}{2}\cdot\frac{1}{a_2} > 1$, and from Lemma 2, we conclude that V_q and consequently e_{qi} converge to zero in fixed-time, with a settling time

$$T_0 \le \frac{2a_2\beta_1^{\frac{1}{a_2}}}{\varsigma_1^{\frac{1}{a_2}}(a_2-1)} + \frac{2a_2\beta_1^{\frac{1}{a_2}}}{(\alpha_1\varsigma_2)^{\frac{1}{a_2}}(a_1-a_2)}. \tag{31}$$

□

Remark 3: It is clear that the settling time is independent of initial conditions $e_{qi}(0)$, that is to say, whatever the initial estimate error $\hat{q}_i - q_d$ is, $\hat{q}_i$ always track q_d in T_0. Similarly, $\hat{v}_i$ also tracks $\dot{q}_d$ in T_0. Therefore, based on the sliding-mode estimator, the attitude state errors can be rewritten as

$$\theta_{1i} = q_i - \hat{q}_i, \tag{32}$$

$$\theta_{2i} = \dot{q}_i - \hat{v}_i, \quad i = 1,\ldots,n. \tag{33}$$

In addition, θ_{1i} and θ_{2i} are equal to e_{1i} and e_{2i} after T_0 respectively. Based on the sliding manifold given by (23), the sliding manifold $s_i \in \mathbb{R}^3$ for the ith spacecraft in the formation is defined as

$$s_i = \mathrm{sig}^{\frac{1}{k_1}}\theta_{2i} + \sigma_{3i}\mathrm{sig}^{p_1}\theta_{1i} + \sigma_{4i}\mathrm{sig}^{g_1}\theta_{1i}, \quad i = 1,\ldots,n, \tag{34}$$

where σ_{3i} and σ_{4i} are positive constants, respectively, $\mathrm{sig}^{p_1}\theta_{1i} = [\mathrm{sig}^{p_1}\theta_{1i1}, \mathrm{sig}^{p_1}\theta_{1i2}, \mathrm{sig}^{p_1}\theta_{1i3}]^{\mathrm{T}}$, $\mathrm{sig}^{\frac{1}{k_1}}\theta_{2i} = \left[\mathrm{sig}^{\frac{1}{k_1}}\theta_{2i1}, \mathrm{sig}^{\frac{1}{k_1}}\theta_{2i2}, \mathrm{sig}^{\frac{1}{k_1}}\theta_{2i3}\right]^{\mathrm{T}}$. After T_0, the sliding manifold s_i is equivalent to

$$s_i = \mathrm{sig}^{\frac{1}{k_1}}e_{2i} + \sigma_{3i}\mathrm{sig}^{p_1}e_{1i} + \sigma_{4i}\mathrm{sig}^{g_1}e_{1i}, \quad i = 1,\ldots,n. \tag{35}$$

3.3. Design and stability analysis of the controller

In this section, the distributed fixed-time controllers will be designed for n rigid spacecraft in the presence of external disturbances, such that attitude errors e_1 and e_2 can converge to small regions in fixed time respectively.

It follows from (8) that $\|g_i\| \le \|T_i\| \cdot \left\|J_i^{-1}\right\| \cdot \|d_i\|$. In addition, according to Assumption 3, (5), and $\|q_i\| \le 1$, we can conclude that there exists a positive but unknown constant η_i such that $\|g_i\| \le \eta_i$. In order to estimate the upper bound parameter η_i, the adaptive update law is introduced as

$$\dot{\hat{\eta}}_i = \frac{1}{2c_i}\left(-2\delta_i\hat{\eta}_i + \frac{1}{k_1}\sum_{m=1}^{3}|\theta_{2im}|^{\frac{1}{k_1}-1}|s_{im}|\right), \quad i = 1,\ldots,n, \tag{36}$$

where $\hat{\eta}_i$ is the estimate of η_i, and $c_i = \frac{\delta_i(2\sigma-1)}{2\sigma}$, $\sigma > 0$, $\delta_i > 0$ are design parameters.

Based on the fixed-time sliding mode, the fixed-time sliding-mode estimator and the adaptive update law, the distributed control law with boundary layer for the ith spacecraft is now given as follows:

$$\begin{aligned} u_i =& J_iP_i\bar{u}_i, \\ \bar{u}_i =& -h_i + \dot{\hat{v}}_i - \sigma_{3i}k_1p_1\mathrm{diag}\left\{\mathrm{sig}^{2-\frac{1}{k_1}}(\theta_{2i})\right\}|\theta_{1i}|^{p_1-1} \\ & - \sigma_{4i}k_1g_1\mathrm{diag}\left\{\mathrm{sig}^{2-\frac{1}{k_1}}(\theta_{2i})\right\}|\theta_{1i}|^{g_1-1} - l_1\mathrm{sig}^{p_2}s_i \\ & - l_2\mathrm{sig}^{g_2}s_i - u_{i\mathrm{adp}}, \end{aligned} \tag{37}$$

where s_i takes the form of (34), $l_1 > 0$, $l_2 > 0$ are the reaching law parameters, p_2, g_2 are positive constants satisfying $p_2 > 1$, $g_2 < 1$, and

$$\begin{aligned} &\mathrm{sig}^{2-\frac{1}{k_1}}(\theta_{2i}) \\ &= \left[\mathrm{sig}^{2-\frac{1}{k_1}}(\theta_{2i1}),\ \mathrm{sig}^{2-\frac{1}{k_1}}(\theta_{2i2}),\ \mathrm{sig}^{2-\frac{1}{k_1}}(\theta_{2i3})\right]^{\mathrm{T}}, \\ &|\theta_{1i}|^{p_1-1} = \left[|\theta_{1i1}|^{p_1-1},\ |\theta_{1i2}|^{p_1-1},\ |\theta_{1i3}|^{p_1-1}\right]^{\mathrm{T}}, \\ &|\theta_{1i}|^{g_1-1} = \left[|\theta_{1i1}|^{g_1-1},\ |\theta_{1i2}|^{g_1-1},\ |\theta_{1i3}|^{g_1-1}\right]^{\mathrm{T}}, \\ &\mathrm{sig}^{p_2}s_i = [\mathrm{sig}^{p_2}s_{i1},\ \mathrm{sig}^{p_2}s_{i2},\ \mathrm{sig}^{p_2}s_{i3}]^{\mathrm{T}}, \\ &\mathrm{sig}^{g_2}s_i = [\mathrm{sig}^{g_2}s_{i1},\ \mathrm{sig}^{g_2}s_{i2},\ \mathrm{sig}^{g_2}s_{i3}]^{\mathrm{T}}. \end{aligned}$$

The adaptive law $u_{i\mathrm{adp}} = [u_{i\mathrm{adp}1},\ u_{i\mathrm{adp}2},\ u_{i\mathrm{adp}3}]^{\mathrm{T}}$ estimates the upper bound parameter of the external disturbances, which is designed as

$$u_{i\mathrm{adp}m} = \begin{cases} \dfrac{s_{im}}{|s_{im}|}\hat{\eta}_i, & |s_{im}| > \varepsilon_i, \\ \dfrac{s_{im}}{\varepsilon_i}|\theta_{2im}|^{\frac{1}{k_1}-1}\hat{\eta}_i^2, & |s_{im}| \le \varepsilon_i, \end{cases} \quad m = 1,2,3, \tag{38}$$

where $\varepsilon_i > 0$ is the design parameter.

Inspired by the controller design of [16, 17] and [28], we can have the following theorem.

Theorem 1: For a group of spacecraft described by (2)-(3), if Assumptions 1-3 are satisfied and the control laws are designed as (37), the sliding manifold s_i will converge to the region $|s_{im}| \le \varphi_i \triangleq \Delta_1 \cup \Delta_2, i = 1,\ldots,n, m = 1,2,3$ in fixed time $T_s = T_0 + T_1$, where T_0 is given in (31), and $T_1 = \max(T_{11}, T_{12})$, $T_{11} = \frac{2}{\tau_m(p_2-1)} + \frac{2^{\frac{g_2+1}{2}}}{\delta_m(1-g_2)}$ and $T_{12} = \frac{1}{l_1(p_2-1)} + \frac{1}{l_2(1-g_2)}$, and

$$\Delta_1 = \min\left(\sqrt{2}\left(\frac{\zeta_0}{\tau_m}\right)^{\frac{1}{p_2+1}}, \sqrt{2}\left(\frac{\zeta_0}{2^{1-\frac{g_2+1}{2}}\delta_m}\right)^{\frac{1}{g_2+1}}\right),$$

$$\Delta_2 = \min\left(\left(\frac{\psi_2}{l_1}\right)^{\frac{1}{p_2}}, \left(\frac{\psi_2}{l_2}\right)^{\frac{1}{g_2}}\right),$$

$$\tau_m = \min\left(2^{\frac{p_2+1}{2}}\tau_{m1}, 1\right),$$

$$\delta_m = \min\left(2^{\frac{g_1+1}{2}} \cdot 3^{\frac{1-g_2}{2}} \tau_{m2}, 1\right),$$
$$\tau_{m1} = \min\left(\frac{l_1}{k_1} |e_{2i}|^{\frac{1}{k_1}-1}\right),$$
$$\tau_{m2} = \min\left(\frac{l_2}{k_1} |e_{2i}|^{\frac{1}{k_1}-1}\right),$$
$$\zeta_0 = \begin{cases} \sigma\delta_i\eta_i^2, \ \ \psi_1 \le \sqrt{\dfrac{1}{c_i}}, \\ \sigma\delta_i\eta_i^2 + (c_i\psi_1^2)^{\frac{g_2+1}{2}} - c_i\psi_1^2, \ \ \psi_1 > \sqrt{\dfrac{1}{c_i}}, \end{cases}$$

where ψ_1, ψ_2 are two small positive constants. Furthermore, the attitude state error e_{1i} and e_{2i} will converge to the regions $|e_{1im}| \le \Phi_i = \Delta_3 \cup \Delta_5$, $|e_{2im}| \le \Delta_4$ in fixed time $T_r = T_s + T_2$, where $T_2 = \frac{1}{\sigma_{3i}^{k_1}(1-p_1k_1)} + \frac{1}{\sigma_{4i}^{k_1}(g_1k_1-1)}$, $\Delta_3 = \min\left(\left(\frac{\mu_i}{\sigma_{3i}}\right)^{\frac{1}{p_1}}, \left(\frac{\mu_i}{\sigma_{4i}}\right)^{\frac{1}{g_1}}\right)$, $\Delta_4 = \Delta_1^{k_1} + \sigma_{3i}^{k_1}(\Delta_3)^{p_1k_1} + \sigma_{4i}^{k_1}(\Delta_3)^{g_1k_1}$, $\Delta_5 = \min\left(\left(\frac{\Delta_2}{\sigma_{3i}}\right)^{\frac{1}{p_1}}, \left(\frac{\Delta_2}{\sigma_{4i}}\right)^{\frac{1}{g_1}}\right)$, $|\mu_i| \le \Delta_1$ is a design parameter.

Proof: With the distributed fixed-time sliding-mode estimators, q_d and $\dot{q}_d$ can be estimated in fixed time, thus θ_{1i} and θ_{2i} are equivalent to e_{1i} and e_{2i} after T_0 respectively. Next we will design distributed attitude control law u_i for (15)-(16). Furthermore, the sliding manifold s_i can be rewritten as (35), and the distributed control law $\bar{u}_i$ can be rewritten as

$$\begin{aligned}\bar{u}_i =& -h_i + \dot{\hat{v}}_i - \sigma_{3i}k_1p_1\mathrm{diag}\left\{\mathrm{sig}^{2-\frac{1}{k_1}}(e_{2i})\right\}|e_{1i}|^{p_1-1} \\ & -\sigma_{4i}k_1g_1\mathrm{diag}\left\{\mathrm{sig}^{2-\frac{1}{k_1}}(e_{2i})\right\}|e_{1i}|^{g_1-1} - l_1\mathrm{sig}^{p_2}s_i \\ & - l_2\mathrm{sig}^{g_2}s_i - u_{i\mathrm{adp}}, \end{aligned} \tag{39}$$

and the corresponding θ_{2i} in (36) and (38) are transformed as e_{2i} after T_0.

For each spacecraft, consider the following Lyapunov function candidate

$$V_i = \frac{1}{2}s_i^{\mathrm{T}}s_i + c_i\tilde{\eta}_i^2, \tag{40}$$

where $\tilde{\eta}_i = \eta_i - \hat{\eta}_i$.

Taking the time derivative of the Lyapunov function V_i, we have

$$\begin{aligned}\dot{V}_i =& s_i^{\mathrm{T}}[-\frac{1}{k_1}\mathrm{diag}\{|e_{2i}|^{\frac{1}{k_1}-1}\}(l_1\mathrm{sig}^{p_2}s_i + l_2\mathrm{sig}^{g_2}s_i) \\ & - \frac{1}{k_1}\mathrm{diag}\{|e_{2i}|^{\frac{1}{k_1}-1}\}u_{i\mathrm{adp}} + \frac{1}{k_1}\mathrm{diag}\{|e_{2i}|^{\frac{1}{k_1}-1}\}g_i] \\ & - 2c_i\tilde{\eta}_i\dot{\hat{\eta}}_i \\ \le& -\frac{l_1}{k_1}\sum_{m=1}^{3}|e_{2im}|^{\frac{1}{k_1}-1}|s_{im}|^{p_2+1} - \frac{1}{k_1}\mathrm{diag}\{|e_{2i}|^{\frac{1}{k_1}-1}\}u_{i\mathrm{adp}} \\ & - \frac{l_2}{k_1}\sum_{m=1}^{3}|e_{2im}|^{\frac{1}{k_1}-1}|s_{im}|^{g_2+1} + \frac{\eta_i}{k_1}\sum_{m=1}^{3}|e_{2im}|^{\frac{1}{k_1}-1}|s_{im}| \\ & - 2c_i\tilde{\eta}_i\dot{\hat{\eta}}_i. \end{aligned} \tag{41}$$

For the case of $|s_{im}| > \varepsilon_i$, substituting $u_{i\mathrm{adp}}$ and (36) into (41) results in

$$\begin{aligned}\dot{V}_i \le& -\frac{l_1}{k_1}\sum_{m=1}^{3}|e_{2im}|^{\frac{1}{k_1}-1}|s_{im}|^{p_2+1} + \frac{\tilde{\eta}_i}{k_1}\sum_{m=1}^{3}|e_{2im}|^{\frac{1}{k_1}-1}|s_{im}| \\ & - \frac{l_2}{k_1}\sum_{m=1}^{3}|e_{2im}|^{\frac{1}{k_1}-1}|s_{im}|^{g_2+1} - \frac{\tilde{\eta}_i}{k_1}\sum_{m=1}^{3}|e_{2im}|^{\frac{1}{k_1}-1}|s_{im}| \\ & + 2\delta_i\tilde{\eta}_i\hat{\eta}_i \\ \le& -\tau_{m1}\cdot 2^{\frac{p_2+1}{2}}\left(\sum_{m=1}^{3}\frac{1}{2}s_{im}^2\right)^{\frac{p_2+1}{2}} - (c_i\tilde{\eta}_i^2)^{\frac{p_2+1}{2}} \\ & - \tau_{m2}\cdot 2^{\frac{g_2+1}{2}}3^{\frac{1-g_2}{2}}\left(\sum_{m=1}^{3}\frac{1}{2}s_{im}^2\right)^{\frac{g_2+1}{2}} - (c_i\tilde{\eta}_i^2)^{\frac{g_2+1}{2}} \\ & + (c_i\tilde{\eta}_i^2)^{\frac{p_2+1}{2}} + (c_i\tilde{\eta}_i^2)^{\frac{g_2+1}{2}} + 2\delta_i\tilde{\eta}_i\hat{\eta}_i \\ \le& -\tau_m V_i^{\frac{p_2+1}{2}} - 2^{\frac{1-g_2}{2}}\delta_m V_i^{\frac{g_2+1}{2}} + \zeta_0. \end{aligned} \tag{42}$$

It follows from Lemma 3 that

$$\delta_i\tilde{\eta}_i\hat{\eta}_i \le -\frac{\delta_i(2\sigma-1)}{2\sigma}\tilde{\eta}_i^2 + \frac{\sigma\delta_i}{2}\eta_i^2, \tag{43}$$

if $\frac{\delta_i(2\sigma-1)}{2\sigma}\tilde{\eta}_i^2 > 1$, that is $c_i\tilde{\eta}_i^2 > 1$, we have

$$\begin{aligned}\zeta_0 =& (c_i\tilde{\eta}_i^2)^{\frac{p_2+1}{2}} + (c_i\tilde{\eta}_i^2)^{\frac{g_2+1}{2}} \\ & - c_i\tilde{\eta}_i^2 + \frac{\sigma\delta_i}{2}\eta_i^2 - c_i\tilde{\eta}_i^2 + \frac{\sigma\delta_i}{2}\eta_i^2 \\ \le& (c_i\tilde{\eta}_i^2)^{\frac{g_2+1}{2}} - c_i\tilde{\eta}_i^2 + \sigma\delta_i\eta_i^2. \end{aligned} \tag{44}$$

Moreover, assume that there exists an unknown constant ψ_1 and a compact set D such that $\{\tilde{\eta}_i \,||\tilde{\eta}_i| \le \psi_1\}$. Then we have

$$\zeta_0 \le \sigma\delta_i\eta_i^2 + (c_i\psi_1^2)^{\frac{g_2+1}{2}} - c_i\psi_1^2, \tag{45}$$

if $\frac{\delta_i(2\sigma-1)}{2\sigma}\tilde{\eta}_i^2 \le 1$, that is $c_i\tilde{\eta}_i^2 \le 1$, we have

$$(c_i\tilde{\eta}_i^2)^{\frac{p_2+1}{2}}\Big|_{c_i\tilde{\eta}_i^2\le 1} < (c_i\tilde{\eta}_i^2)^{\frac{p_2+1}{2}}\Big|_{c_i\tilde{\eta}_i^2>1}. \tag{46}$$

So

$$\begin{aligned}\zeta_0 =& (c_i\tilde{\eta}_i^2)^{\frac{p_2+1}{2}} + (c_i\tilde{\eta}_i^2)^{\frac{g_2+1}{2}} \\ & - c_i\tilde{\eta}_i^2 + \frac{\sigma\delta_i}{2}\eta_i^2 - c_i\tilde{\eta}_i^2 + \frac{\sigma\delta_i}{2}\eta_i^2 \\ \le& \sigma\delta_i\eta_i^2. \end{aligned} \tag{47}$$

Then, we have

$$\dot{V}_i \le -\tau_m V_i^{\frac{p_2+1}{2}} - 2^{1-\frac{g_2+1}{2}}\delta_m V_i^{\frac{g_2+1}{2}} + \zeta_0, \tag{48}$$

where

$$\zeta_0 = \begin{cases} \sigma\delta_i\eta_i^2, \ \ \psi_1 \le \sqrt{\dfrac{1}{c_i}}, \\ \sigma\delta_i\eta_i^2 + (c_i\psi_1^2)^{\frac{g_2+1}{2}} - c_i\psi_1^2, \ \ \psi_1 > \sqrt{\dfrac{1}{c_i}}. \end{cases}$$

For the case of $|s_{im}| < \varepsilon_i$, substituting $u_{i\text{adp}}$ and (36) into (41) results in

$$\begin{aligned}\dot{V}_i \le & -\frac{l_1}{k_1}\sum_{m=1}^{3}|e_{2im}|^{\frac{1}{k_1}-1}|s_{im}|^{p_2+1} \\ & -\frac{l_2}{k_1}\sum_{m=1}^{3}|e_{2im}|^{\frac{1}{k_1}-1}|s_{im}|^{g_2+1} \\ & -\frac{\hat{\eta}_i^2}{k_1\varepsilon_i}\sum_{m=1}^{3}s_{im}^2\left(|e_{2im}|^{\frac{1}{k_1}-1}\right)^2 \\ & +\frac{\eta_i}{k_1}\sum_{m=1}^{3}|e_{2im}|^{\frac{1}{k_1}-1}|s_{im}| \\ & -\tilde{\eta}_i\left(-2\delta_i\tilde{\eta}_i+\frac{1}{k_1}\sum_{m=1}^{3}|e_{2im}|^{\frac{1}{k_1}-1}|s_{im}|\right) \\ = & -\frac{l_1}{k_1}\sum_{m=1}^{3}|e_{2im}|^{\frac{1}{k_1}-1}|s_{im}|^{p_2+1} \\ & -\frac{l_2}{k_1}\sum_{m=1}^{3}|e_{2im}|^{\frac{1}{k_1}-1}|s_{im}|^{g_2+1} \\ & -\frac{1}{k_1}\sum_{m=1}^{3}\left(\frac{\hat{\eta}_i|s_{im}|\cdot|e_{2im}|^{\frac{1}{k_1}-1}}{\sqrt{\varepsilon_i}}-\frac{\sqrt{\varepsilon_i}}{2}\right)^2 \\ & +\frac{3\varepsilon_i}{4k_1}+2\delta_i\tilde{\eta}_i\hat{\eta}_i \\ \le & -\tau_m V_i^{\frac{p_2+1}{2}}-2^{\frac{1-g_2}{2}}\delta_m V_i^{\frac{g_2+1}{2}}+\zeta_1. \end{aligned} \tag{49}$$

So

$$\zeta_1=\zeta_0+\frac{3\varepsilon_i}{4k_1}>\zeta_0. \tag{50}$$

Therefore, according to the analysis of two cases, we can obtain

$$\dot{V}_i \le -\tau_m V_i^{\frac{p_2+1}{2}}-2^{\frac{1-g_2}{2}}\delta_m V_i^{\frac{g_2+1}{2}}+\zeta_0. \tag{51}$$

Then, equation (51) can be rewritten as the following two forms:

$$\dot{V}_i \le -\left(\tau_m-\frac{\zeta_0}{V_i^{\frac{p_2+1}{2}}}\right)V_i^{\frac{p_2+1}{2}}-2^{\frac{1-g_2}{2}}\delta_m V_i^{\frac{g_2+1}{2}}, \tag{52}$$

$$\dot{V}_i \le -\tau_m V_i^{\frac{p_2+1}{2}}-\left(2^{\frac{1-g_2}{2}}\delta_m-\frac{\zeta_0}{V_i^{\frac{g_2+1}{2}}}\right)V_i^{\frac{g_2+1}{2}}. \tag{53}$$

Similar to the analysis of [16, 17] and [28], next it will be discussed in two cases.

Case 1: For the case $e_{2im}\neq 0$, from (52) if $\tau_m-\frac{\zeta_0}{V_i^{\frac{p_2+1}{2}}}>0$, then the fixed-time stability is still guaranteed, and hence, by using Lemma 2, the sliding manifold s_i for ith spacecraft will converge to the region

$$|s_{im}|\le\sqrt{2}\left(\frac{\zeta_0}{\tau_m}\right)^{\frac{1}{p_2+1}} \tag{54}$$

in fixed time $T_{11}=\frac{2}{\tau_m(p_2-1)}+\frac{2^{\frac{g_2+1}{2}}}{\delta_m(1-g_2)}$. From (53) if $2^{\frac{1-g_2}{2}}\delta_m-\frac{\zeta_0}{V_i^{\frac{g_2+1}{2}}}>0$, then the sliding manifold s_i for ith spacecraft will converge to the region

$$|s_{im}|\le\sqrt{2}\left(\frac{\zeta_0}{2^{1-\frac{g_2+1}{2}}\delta_m}\right)^{\frac{1}{g_2+1}} \tag{55}$$

in fixed time T_{11}. Therefore all the sliding modes s_i can converge to the region $|s_{im}|\le\Delta_1$ in fixed time T_{11}, with

$$\Delta_1=\min\left(\sqrt{2}\left(\frac{\zeta_0}{\tau_m}\right)^{\frac{1}{p_2+1}},\sqrt{2}\left(\frac{\zeta_0}{2^{1-\frac{g_2+1}{2}}\delta_m}\right)^{\frac{1}{g_2+1}}\right).$$

Case 2: For the case $e_{2im}=0$, $\bar{u}_i$ degenerates into the following form

$$\bar{u}_i=-h_i+\dot{\hat{v}}_i-l_1\text{sig}^{p_2}s_i-l_2\text{sig}^{g_2}s_i-u_{i\text{adp}}. \tag{56}$$

Substituting (56) into (16), we have

$$\dot{e}_{2i}=-l_1\text{sig}^{p_2}s_i-l_2\text{sig}^{g_2}s_i-u_{i\text{adp}}+g_i. \tag{57}$$

Let $\bar{g}_i=g_i-u_{i\text{adp}}$, the upper bound of $\bar{g}_{im}$ is assumed as ψ_2, i.e., $|\bar{g}_{im}|\le\psi_2$. Then we have $|s_{im}|<(\frac{\psi_2}{l_1})^{\frac{1}{p_2}}$ or $|s_{im}|<(\frac{\psi_2}{l_2})^{\frac{1}{g_2}}$ in fixed time $T_{12}=\frac{1}{l_1(p_2-1)}+\frac{1}{l_2(1-g_2)}$. Furthermore, for any $e_{2im}=0$ and $s_{im}\notin(|s_{im}|\le\Delta_2)$, it follows that $\dot{e}_{2im}\neq 0$.

Therefore, according to the analysis of Case 1 and Case 2, once $s_{im}\notin(|s_{im}|\le\Delta_1\cup\Delta_2)$, all the sliding modes s_i can converge to the region $|s_{im}|\le\varphi_i$ in fixed time $T_1=\max(T_{11},T_{12})$.

For the case $e_{2im}\neq 0$, $|s_{im}|\le\Delta_1$, from (35), we conclude that

$$\text{sig}^{\frac{1}{k_1}}e_{2im}+\sigma_{3i}\text{sig}^{p_1}e_{1im}+\sigma_{4i}\text{sig}^{g_1}e_{1im}=\mu_i,\quad|\mu_i|\le\Delta_1. \tag{58}$$

The preceding equation can be rewritten in the following two forms:

$$\begin{aligned}&\text{sig}^{\frac{1}{k_1}}e_{2im}+\left(\sigma_{3i}-\frac{\mu_i}{\text{sig}^{p_1}e_{1im}}\right)\text{sig}^{p_1}e_{1im} \\ &\quad+\sigma_{4i}\text{sig}^{g_1}e_{1im}=0, \end{aligned} \tag{59}$$

$$\begin{aligned}&\text{sig}^{\frac{1}{k_1}}e_{2im}+\sigma_{3i}\text{sig}^{p_1}e_{1im} \\ &\quad+\left(\sigma_{4i}-\frac{\mu_i}{\text{sig}^{g_1}e_{1im}}\right)\text{sig}^{g_1}e_{1im}=0. \end{aligned} \tag{60}$$

From (59), if $\sigma_{3i}-\frac{\mu_i}{\text{sig}^{p_1}e_{1im}}>0$, then the fixed-time-based SM is still kept, and hence, the state error e_{1i} for ith spacecraft will converge to the region

$$|e_{1im}|<\left(\frac{\mu_i}{\sigma_{3i}}\right)^{\frac{1}{p_1}} \tag{61}$$

in fixed time $T_2 = \frac{1}{\sigma_{3i}^{k_1}(1-p_1k_1)} + \frac{1}{\sigma_{4i}^{k_1}(g_1k_1-1)}$. From (60), if $\sigma_{4i} - \frac{\mu_i}{\text{sig}^{g_1} e_{1im}} > 0$, then the fixed-time-based SM is still kept, and hence, the state error e_{1i} for ith spacecraft will converge to the region

$$|e_{1im}| < \left(\frac{\mu_i}{\sigma_{4i}}\right)^{\frac{1}{g_1}} \tag{62}$$

in fixed time T_2. Therefore, the state error e_{1i} will converge to the region $\Delta_3 = \min\left(\left(\frac{\mu_i}{\sigma_{3i}}\right)^{\frac{1}{p_1}}, \left(\frac{\mu_i}{\sigma_{4i}}\right)^{\frac{1}{g_1}}\right)$ in fixed time T_2. Furthermore, the state error e_{2i} converge to the region

$$|e_{2im}| \le \Delta_1^{k_1} + \sigma_{3i}^{k_1}(\Delta_3)^{p_1k_1} + \sigma_{4i}^{k_1}(\Delta_3)^{g_1k_1} = \Delta_4 \tag{63}$$

in fixed time T_2.

For $e_{2im} = 0$, $|s_{im}| \le \Delta_2$, the state error e_{1i} will converge to the region

$$|e_{1im}| \le \min\left(\left(\frac{\Delta_2}{\sigma_{3i}}\right)^{\frac{1}{p_1}}, \left(\frac{\Delta_2}{\sigma_{4i}}\right)^{\frac{1}{g_1}}\right) = \Delta_5. \tag{64}$$

Therefore, according to the analysis of two cases, the state error e_{1i} and the state error e_{2i} will converge to the region $|e_{1im}| \le \Phi_i = \Delta_3 \cup \Delta_5$ and the region $|e_{2im}| \le \Delta_4$ in fixed time T_2.

From the above analysis, we conclude that using the distributed fixed-time sliding-mode estimators (26)-(27) and the control input (37), the sliding manifold s_i will converge to the region $|s_{im}| \le \varphi_i \triangleq \Delta_1 \cup \Delta_2$ in fixed time $T_s = T_0 + T_1$, furthermore, the attitude state error e_{1i} and e_{2i} will converge to the regions $|e_{1im}| \le \Phi_i = \Delta_3 \cup \Delta_5$, $|e_{2im}| \le \Delta_4$ in fixed time $T_r = T_s + T_2$.

The proof is completed. □

Remark 4: Since the sliding mode estimator is employed in the design of controller, the adaptation law is only required to estimate the upper bound parameter of external disturbances existing in each spacecraft itself. In contrast to estimating the upper bound parameter of total external disturbances $\left\|\sum_{j=1}^{n} l_{ij}g_j + b_ig_i\right\|$ in [17], the adaptation law in the proposed controller only estimates $\|g_i\|$ for each spacecraft. Since the upper bound of estimation is largely decreased, the convergence rate and estimate accuracy of the closed-loop system are improved.

Remark 5: Based on the fixed-time sliding mode and sliding-mode estimator, this paper proposes the distributed fixed-time control laws. Compared with [19], the constructed sliding-mode estimators (26) and (27) provide fixed settling time independent of initial conditions, which improves the convergence rate especially when the initial state is far away from the equilibrium. Furthermore, in contrast to the dynamics without disturbances in [19], our paper studies the synchronization problem of multi-spacecraft systems with external disturbances. Compared with [17], the proposed control laws (37) have the following advantages: First, all the follower spacecraft in [17] need the real time state information q_d and $\dot{q}_d$ of the leader, while our controller based on fixed-time sliding-mode estimator only requires that the followers connected to the leader directly can get the real time state of the leader and meanwhile other followers only require the constant upper bound of the leader's state, which reduces the communication interaction between each spacecraft; second, the control laws (37) require no input information of the neighbour spacecraft, therefore avoid the algebraic loop problem; third, the tracking errors converge to the regions in fixed time independent of initial states.

4. SIMULATION RESULTS

In this section, numerical simulations are carried out to verify the effectiveness of the proposed fixed-time SM and attitude synchronization control strategy. Firstly, comparisons are made to show the faster convergence of Fixed-time SM. Then, we compare the performance of the proposed sliding-mode estimator and the finite-time sliding-mode estimator. Thirdly, simulations for comparisons of convergence rate and performance of the control laws are given.

In the simulation, we consider a scenario with four follower spacecraft which are governed by (2)-(3) and one virtual leader. The communication topology for four spacecraft and the virtual leader is shown in Fig. 1, thus corresponding Laplacian matrix L and leader adjacency matrix B can be respectively described as:

$$L = \begin{bmatrix} 2 & -1 & -1 & 0 \\ -1 & 2 & 0 & -1 \\ -1 & 0 & 2 & -1 \\ 0 & -1 & -1 & 2 \end{bmatrix},$$

and $B = \text{diag}\{1,1,0,0\}$. The spacecraft in the formation are considered to nanosatellites, the inertia matrix for each spacecraft is chosen from [32]

$$J_1 = [1\ 0.1\ 0.1; 0.1\ 0.1\ 0.1; 0.1\ 0.1\ 0.9]\ \text{kg}\cdot\text{m}^2,$$
$$J_2 = [1.5\ 0.2\ 0.3; 0.2\ 0.9\ 0.4; 0.3\ 0.4\ 2.0]\ \text{kg}\cdot\text{m}^2,$$
$$J_3 = [0.8\ 0.1\ 0.2; 0.1\ 0.7\ 0.3; 0.2\ 0.3\ 1.1]\ \text{kg}\cdot\text{m}^2,$$
$$J_4 = [1.2\ 0.3\ 0.7; 0.3\ 0.9\ 0.2; 0.7\ 0.2\ 1.4]\ \text{kg}\cdot\text{m}^2.$$

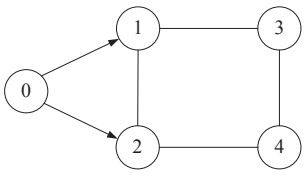

Fig. 1. Communication topology for spacecraft formation.

Table 1. Initial states and parameters of estimators.

Parameter name	Value
Initial states	$\hat{q}_1 = [0,-0.2,0]^{\mathrm{T}}$
	$\hat{q}_2 = [0.4,0.2,0.6]^{\mathrm{T}}$
	$\hat{q}_3 = [0.1,0.1,0.15]^{\mathrm{T}}$
	$\hat{q}_4 = [0.3,-0.08,0.45]^{\mathrm{T}}$
	$\hat{v}_1 = [-0.1,0.05,0.15]^{\mathrm{T}}$
	$\hat{v}_2 = [0.1,0,0.3]^{\mathrm{T}}$
	$\hat{v}_3 = [-0.05,0.2,-0.2]^{\mathrm{T}}$
	$\hat{v}_4 = [0.04,-0.04,-0.1]^{\mathrm{T}}$
Desired trajectory	$q_d = [0.2\cos(0.5t),0.2\sin(0.5t),0.3]^{\mathrm{T}}$
Estimator parameters	$a_1 = 2, a_2 = \frac{5}{3},$
	$\alpha_1 = \beta_1 = 1,$
	$\lambda_1 = 0.05, \lambda_2 = 0.06$

Table 2. Numerical simulation parameters.

Parameter name	Value
Initial states	$q_1(0) = [2.2,2.0,-2.2]^{\mathrm{T}}$
	$q_2(0) = [-1.9,2.0,2.9]^{\mathrm{T}}$
	$q_3(0) = [-1.9,-2.3,2.55]^{\mathrm{T}}$
	$q_4(0) = [-1.5,2.72,-1.25]^{\mathrm{T}}$
Initial angular velocity	$\omega_i(0) = [0,0,0]^{\mathrm{T}}, i = 1,\ldots,4$
External disturbance	$d_i = 0.01\,[\sin(2t),\cos(2t),\sin(4t)]^{\mathrm{T}}$
Control parameters	$\sigma_{3i} = \sigma_{4i} = 0.3,$
	$k_1 = \frac{3}{5}, \varepsilon_i = 0.5$
	$p_1 = \frac{7}{5}, g_1 = \frac{7}{3}$
	$p_2 = \frac{9}{7}, g_2 = \frac{3}{5}$
	$l_1 = 0.5, l_2 = 0.5$
	$\delta_i = 2, \sigma = 1$
	$\hat{\eta}_i(0) = 0, i = 1,\ldots,4$

The initial states and numerical parameters of the fixed-time sliding-mode estimator are selected in Table 1. The initial attitude of each spacecraft in the formation and other numerical parameters are given in Table 2.

4.1. Faster convergence illustration of fixed-time SM

In order to verify the faster convergence performance of fixed-time SM comparing with FTSM and NFTSM, we consider the following sliding modes:

$$\text{FTSM: } s_1 = \dot{x}_1 + x_1 + \mathrm{sig}^{\frac{3}{5}} x_1,$$

$$\text{NFTSM: } s_2 = x_2 + 0.01\mathrm{sig}^{\frac{7}{3}} x_2 + 0.01\mathrm{sig}^{\frac{5}{3}} \dot{x}_2,$$

$$\text{Fixed-timeSM: } s_3 = \mathrm{sig}^{\frac{5}{3}} \dot{x}_3 + 100\mathrm{sig}^{\frac{7}{5}} x_3 + \mathrm{sig}^{\frac{7}{3}} x_3$$

with the initial state $x_i(0) = 20$ and $x_i(0) = 200$, $i = 1, 2, 3$. Let all above sliding modes equal to zero, then we have

$$\text{FTSM: } \dot{x}_1 = -\mathrm{sig}^{\frac{3}{5}} x_1 - x_1,$$

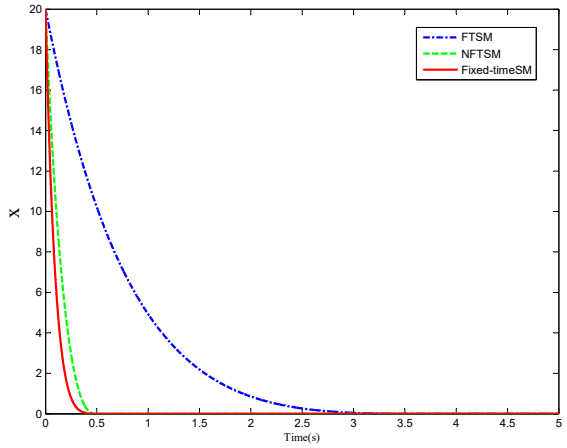

Fig. 2. Comparison of FTSM, NFTSM and fixed-time SM when $x(0) = 20$.

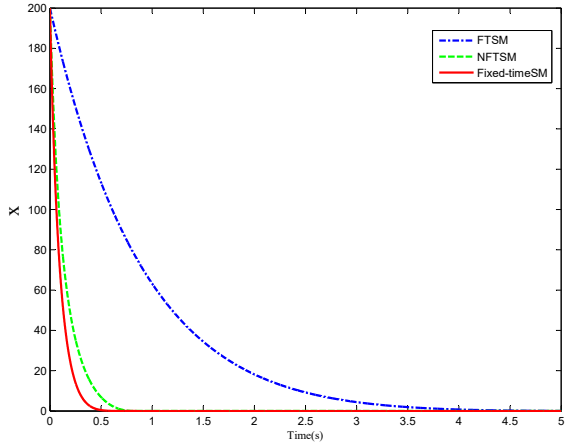

Fig. 3. Comparison of FTSM, NFTSM and fixed-time SM when $x(0) = 200$.

$$\text{NFTSM: } \dot{x}_2 = -\mathrm{sig}^{\frac{3}{5}} \left(100x_2 + \mathrm{sig}^{\frac{7}{3}} x_2\right),$$

$$\text{Fixed-timeSM: } \dot{x}_3 = -\mathrm{sig}^{\frac{3}{5}} \left(100\mathrm{sig}^{\frac{7}{5}} x_3 + \mathrm{sig}^{\frac{7}{3}} x_3\right).$$

The convergence curves of FTSM, NFTSM and fixed-time SM are shown in Fig. 2 and Fig. 3 when the initial states are 20 and 200 respectively. It can be seen from Fig. 2 and Fig. 3 that fixed-time SM have better convergence rate than FTSM and NFTSM. Furthermore, whatever the initial state is, the initial state of fixed-time SM can converge to zero in $0.6s$, implying that the upper bound of the settling time is independent of the initial state.

4.2. Fixed-time tracking of sliding-mode estimator

In this section, the performance comparison between the proposed sliding-mode estimators and the finite-time sliding-mode estimators is studied. For this example, the finite-time sliding-mode estimators proposed in [33] are

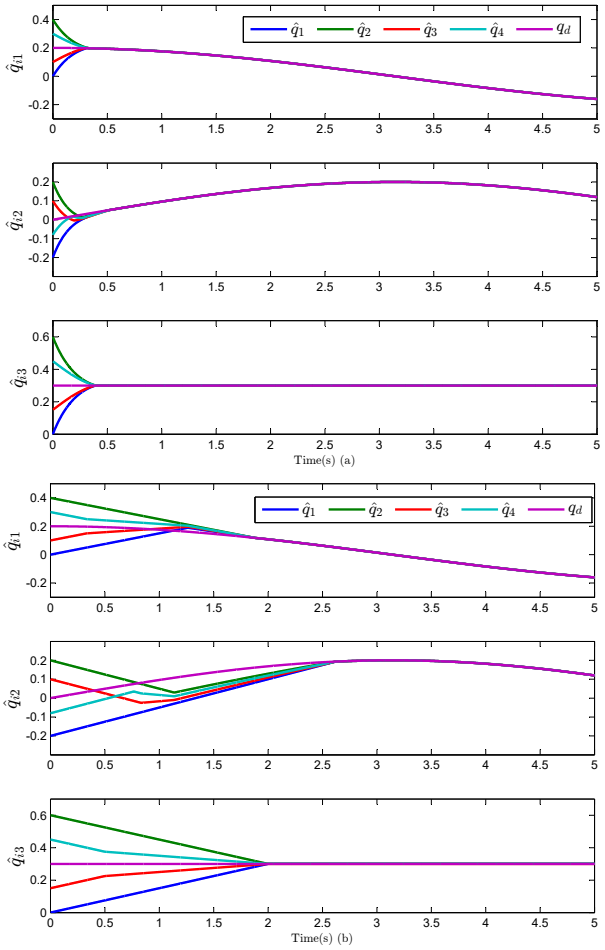

Fig. 4. The estimates of q_d. (a) Fixed-time sliding-mode estimator in (26). (b) Finite-time sliding-mode estimator in [33].

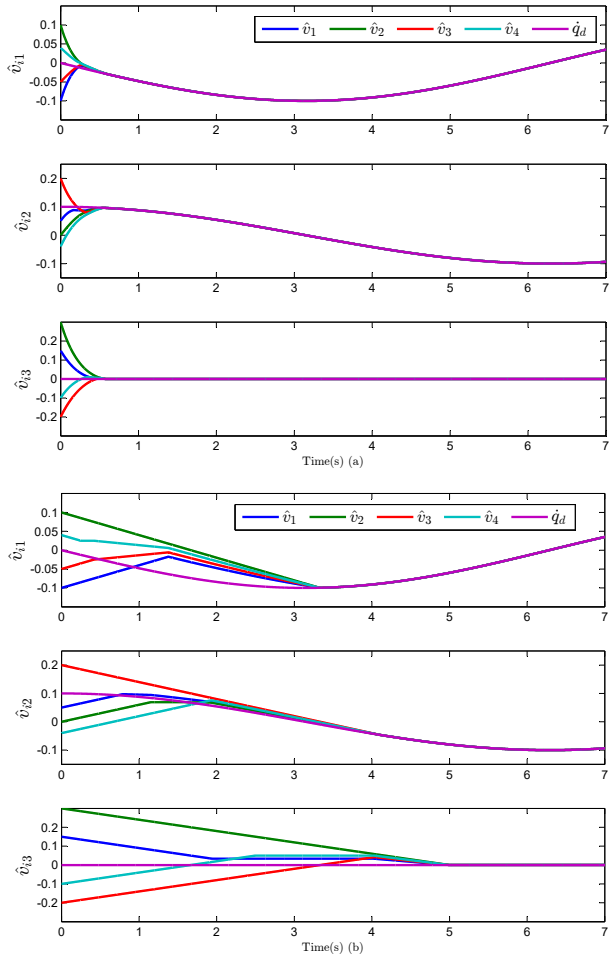

Fig. 5. The estimates of $\dot{q}_d$. (a) Fixed-time sliding-mode estimator in (27). (b) Finite-time sliding-mode estimator in [33].

defined as

$$\dot{\hat{q}}_i = -\lambda_1 \text{sign}\left[\sum_{j\in N_i} a_{ij}(\hat{q}_i - \hat{q}_j) + b_i(\hat{q}_i - q_d)\right], \quad (65)$$

$$\dot{\hat{v}}_i = -\lambda_2 \text{sign}\left[\sum_{j\in N_i} a_{ij}(\hat{v}_i - \hat{v}_j) + b_i(\hat{v}_i - \dot{q}_d)\right]. \quad (66)$$

All parameters of the finite-time sliding-mode estimators are chosen the same as those given in Table 1. It can be seen from Fig. 4 and Fig. 5 that the estimates $\hat{q}_i$ and $\hat{v}_i$ of our sliding-mode estimators precisely coincide with q_d and $\dot{q}_d$ in 1 s, while the estimates $\hat{q}_i$ and $\hat{v}_i$ in (65) and (66) coincide with q_d and $\dot{q}_d$ in 5 s approximately. The simulation results validate the faster convergence performance of the fixed-time sliding-mode estimators comparing with the sliding-mode estimators in [33].

4.3. Simulations for attitude synchronization

In this section, simulations for attitude synchronization are given. With the proposed controller (39), the response curves are shown in Fig. 6 and Fig. 7. Fig. 6 shows the response curves of attitude tracking errors e_{1i} ($i = 1, \ldots, 4$) for each spacecraft. It is clear that all attitude tracking errors converge to the neighborhood around zero in fixed time even in the presence of external disturbances, which validates the effectiveness of the controller (39). The response curves of control torque for each spacecraft are shown in Fig. 7. It is observed that chattering is avoided since the bounded-layer is implemented. These simulation results imply that the proposed controller (39) provide the fixed time control and good robustness.

In order to investigate the performance of the proposed controller on attitude synchronization, station-keeping attitude error and overall control effort metrics are employed. The station-keeping attitude error metric (SKAEM) is defined as [14]

$$\text{SKAEM} = \sqrt{\sum_{i=1}^{n} \|e_{1i}\|^2}, \quad (67)$$

and the overall control effort metric (OCEM) exerted by the spacecraft in the formation is defined as

$$\text{OCEM} = \sqrt{\sum_{i=1}^{n} \|u_i\|^2}. \tag{68}$$

In order to meet the spacecraft application requirements, we consider the multiple rigid spacecraft system under actuator saturation, and the dynamic (2) for the ith spacecraft is expressed as

$$J_i \dot{\omega}_i = -\omega_i^{\times} J_i \omega_i + \text{sat}(u_i) + d_i, \quad i = 1, \ldots, n, \tag{69}$$

where $\text{sat}(u_i) = [\text{sat}(u_{i1}), \text{sat}(u_{i2}), \text{sat}(u_{i3})]^{\text{T}}$ is the vector of actual control torque and $\text{sat}(u_{im})$ $(m = 1, 2, 3)$ is defined as

$$\text{sat}(u_{im}) = \begin{cases} \Theta, \text{ if } u_{im} > \Theta, \\ u_{im}, \text{ if } |u_{im}| \le \Theta, \\ -\Theta, \text{ if } u_{im} < -\Theta, \end{cases}$$

with the input limit $\Theta = 1$ Nm.

For the multiple spacecraft system under actuator saturation (69), the performance of the proposed controller, the NFTSM-based controller (NFTSMC) and the FTSM-based controller (FTSMC) are compared next. For this example, the NFTSM s_i is defined as

$$s_i = e_{1i} + \sigma_{3i} \text{sig}^{g_1} e_{1i} + \sigma_{4i} \text{sig}^{\frac{1}{k_1}} e_{2i}, \tag{70}$$

and the FTSM s_i is defined as

$$s_i = e_{2i} + \sigma_{3i} e_{1i} + \sigma_{4i} \text{sig}^{k_1} e_{1i}. \tag{71}$$

All parameters of the NFTSM and the FTSM are chosen as the same as those given in Table 1 and 2, and the corresponding distributed controllers are chosen as those in [17] and [14]. The response of SKAEM and OCEM for the proposed controller, the NFTSMC and the FTSMC are shown in Fig. 8 and Fig. 9. It can be seen that the fixed-time-based controller can provide faster convergence and higher attitude synchronization performance than the NFTSM-based controller and the FTSM-based controller.

5. CONCLUSION

In this paper, the distributed fixed-time attitude synchronization control problem is studied using fixed-time-based TSM associated with sliding-mode estimators. A novel fixed-time TSM is constructed based on the attitude state error for each spacecraft, whose settling time is independent of initial conditions. Then, based on the fixed-time sliding-mode estimators, the distributed adaptive controllers with boundary layer are proposed, which can force the attitude state errors to small regions containing the origin in fixed time. Moreover, the proposed controllers are chattering free and avoid the algebraic loop

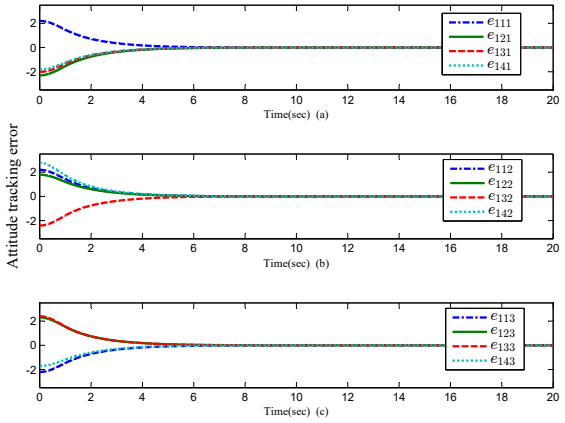

Fig. 6. Attitude tracking errors. (a) e_{1i1}, (b) e_{1i2}, (c) e_{1i3} $(i = 1, \ldots, 4)$.

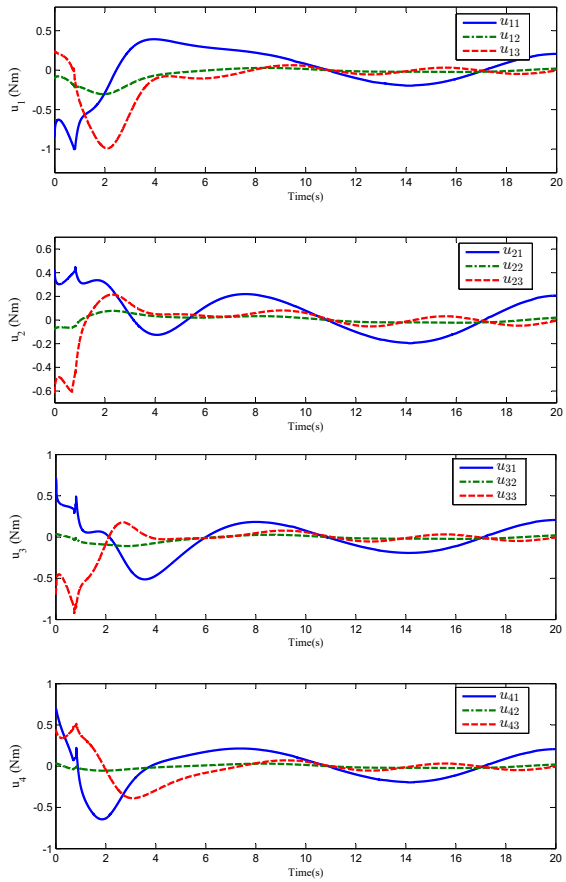

Fig. 7. Response curves of u_i $(i = 1, 2, 3, 4)$.

problem. The performance of the proposed controller is examined through numerical simulation, which shows that the proposed controller can provide faster convergence and higher accuracy than the existing controller. In future work, the extension of the fixed-time controller to output feedback control without velocity measurements will be

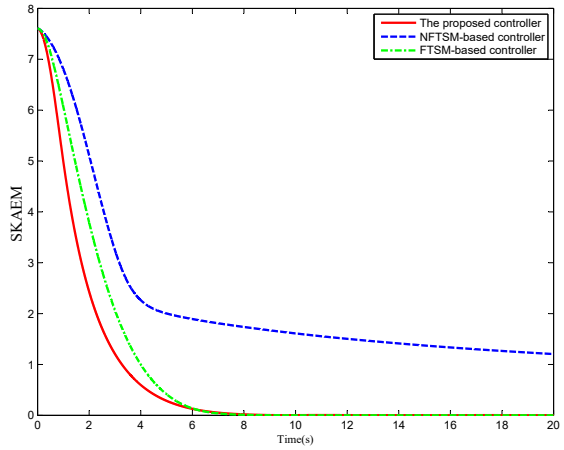

Fig. 8. Performance comparison: SKAEM

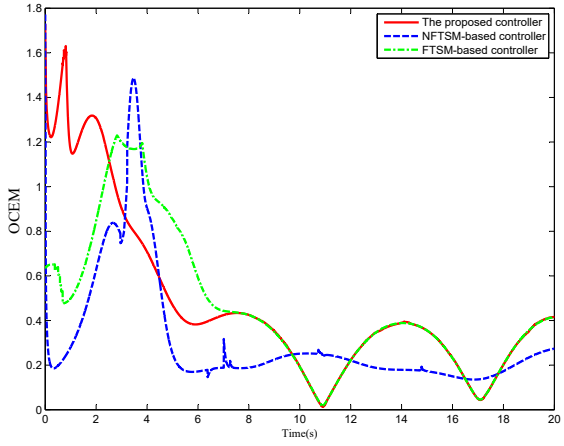

Fig. 9. Performance comparison: OCEM

investigated.

REFERENCES

[1] J. Y. Tien, J. M. Srinivasan, L. E. Young, and G. H. Purcell, "Formation acquisition sensor for the terrestrial planet finder (TPF) mission," *Proc. of the 2004 IEEE Aerospace Conference*, pp. 2680-2690, 2004.

[2] W. H. Kang and H. Yeh, "Coordinated attitude control of multisatellite systems," *International Journal of Robust and Nonlinear Control*, vol. 12, pp. 185-205, 2002.

[3] D. V. Dimarogonas, P. Tsiotras, and K. J. Kyriakopoulos, "Leader-follower cooperative attitude control of multiple rigid bodies," *Systems & Control Letters*, vol. 58, no. 6, pp. 429-435, June 2009.

[4] A. Abdessameud and A. Tayebi, "Attitude synchronization of a group of spacecraft without velocity measurements," *IEEE Trans. on Automatic Control*, vol. 54, no. 11, pp. 2642-2648, November 2009.

[5] A. M. Zou, K. D. Kumar, and Z. G. Hou, "Attitude coordination control for a group of spacecraft without velocity measurements," *IEEE Trans. on Control Systems Technology*, vol. 20, no. 5, pp. 1160-1174, September 2012.

[6] A. Abdessameud, A. Tayebi, and I. G. Polushin, "Attitude synchronization of multiple rigid bodies with communication delays," *IEEE Trans. on Automatic Control*, vol. 57, no. 9, pp. 2405-2411, September 2012.

[7] A. M. Zou and K. D. Kumar, "Neural network-based distributed attitude coordination control for spacecraft formation flying with input saturation," *IEEE Trans. on Neural Networks and Learning Systems*, vol. 23, no. 7, pp. 1155-1162, July 2012.

[8] Z. Zhu, Y. Xia, and M. Fu, "Attitude stabilization of rigid spacecraft with finite-time convergence," *International Journal of Robust and Nonlinear Control*, vol. 21, no. 6, pp. 686-702, April 2011.

[9] K. Lu and Y. Xia, "Adaptive attitude tracking control for rigid spacecraft with finite-time convergence," *Automatica*, vol. 49, no. 12, pp. 3591-3599, December 2013.

[10] E. D. Jin and Z. W. Sun, "Robust controllers design with finite time convergence for rigid spacecraft attitude tracking control," *Aerospace Science and Technology*, vol. 12, no. 4, pp. 324-330, June 2008.

[11] H. Liang, Z. Sun, and J. Wang, "Finite-time attitude synchronization controllers design for spacecraft formations via behavior-based approach," *Proceedings of the Institution of Mechanical Engineers Part G: Journal of Aerospace Engineering*, vol. 227, no. 11, pp. 1737-1753, November 2013.

[12] H. Liang, Z. Sun, and J. Wang, "Robust decentralized attitude control of spacecraft formations under time-varying topologies, model uncertainties and disturbances," *Acta Astronautica*, vol. 81, no. 2, pp. 445-455, December 2012.

[13] X. Yu and Z. Man, "Fast terminal sliding-mode control design for nonlinear dynamical systems," *IEEE Trans. on Circuits and Systems I*, vol. 49, no. 2, pp. 261-264, February 2002.

[14] A. M. Zou and K. Kumar, "Distributed attitude coordination control for spacecraft formation flying," *IEEE Trans. on Aerospace Electronic Systems*, vol. 48, no. 2, pp. 1329-1346, April 2012.

[15] L. Yang and J. Y. Yang, "Nonsingular fast terminal sliding-mode control for nonlinear dynamical systems," *International Journal of Robust and Nonlinear Control*, vol. 21, no. 16, pp. 1865-1879, November 2011.

[16] S. H. Yu, X. H. Yu, B. Shirinzadeh, and Z. H. Man, "Continuous finite-time control for robotic manipulators with terminal sliding mode," *Automatica*, vol. 41, no. 11, pp. 1957-1964, November 2005.

[17] L. Zhao and Y. M. Jia, "Decentralized adaptive attitude synchronization control for spacecraft formation using nonsingular fast terminal sliding mode," *Nonlinear Dynamics*, vol. 78, no. 4, pp. 2779-2794, December 2014.

[18] A. Polyakov, "Nonlinear feedback design for fixed-time stabilization of linear control systems," *IEEE Trans. on Automatic Control*, vol. 57, no. 8, pp. 2106-2110, August 2012.

[19] L. Ma, S. Wang, H. Min, Y. Liu, and S. Liao, "Distributed finite-time attitude dynamic tracking control for multiple rigid spacecraft," *IET Control Theory & Applications*, vol. 9, no. 17, pp. 2568-2573, November 2015.

[20] P. C. Huges, *Spacecraft Attitude Dynamics*, Wiley, Hoboken, 1986.

[21] H. Schaub, M. R. Akella, and J. L. Junkins, "Adaptive control of nonlinear attitude motions realizing linear closed loop dynamics," *Journal of Guidance Control and Dynamics*, vol. 24, no. 1, pp. 95-100, January-February 2001.

[22] J. J. E. Slotine and M. D. D. Benedetto, "Hamiltonian adaptive control of spacecraft," *IEEE Trans. on Automatic Control*, vol. 35, no. 7, pp. 848-852, July 1990.

[23] A. F. Filippov, *Differential Equations with Discontinuous Right-Hand Sides*, Kluwer Academic, New York, 1988.

[24] C. Song, S. J. Kim, S. H. Kim, and H. S. Nam, "Robust control of the missile attitude based on quaternion feedback," *Control Engineering Practice*, vol. 14, no. 7, pp. 811-818, July 2006.

[25] Z. Y. Zuo and L. Tie, "A new class of finite-time nonlinear consensus protocols for multi-agent systems," *International Journal of Control*, vol. 87, no. 2, pp. 363-370, February 2014.

[26] Z. Y. Zuo, "Non-singular fixed-time terminal sliding mode control of non-linear systems," *IET Control Theory & Applications*, vol. 9, no. 4, pp. 545-552, February 2015.

[27] S. Parsegov, A. Polyakov, and P. Shcherbakov, "Nonlinear fixed-time control protocol for uniform allocation of agents on a segment," *Proc. of the 51st Conf. Decision and Control*, pp. 7732-7737, 2012.

[28] K. F. Lu and Y. Q. Xia, "Finite-time attitude stabilization for rigid spacecraft," *International Journal of Robust and Nonlinear Control*, vol. 25, no. 1, pp. 32-51, January 2015.

[29] M. Abramowitz and IA. Stegun, *Handbook of Mathematical Functions: with Formulas, Graphs, and Mathematical Tables*, Dover, New York, 1972.

[30] J. J. Fu and J. Z. Wang, "Fixed-time coordinated tracking for second-order multi-agent systems with bounded input uncertainties," *Systems & Control Letters*, vol. 93, pp. 1-12, July 2016.

[31] S. Y. Khoo, L. H. Xie, and Z. H. Man, "Robust finite-time consensus tracking algorithm for multirobot systems," *IEEE Trans. on Mechatronics*, vol. 14, no. 2, pp. 219-228, April 2009.

[32] W. Ren, "Distributed attitude alignment in spacecraft formation flying," *International Journal of Adaptive Control and Signal Processing*, vol. 21, no. 2-3, pp. 95-113, March-April 2007.

[33] J. K. Zhou, Q. L. Hu, and M. I. Friswell, "Decentralized finite time attitude synchronization control of satellite formation flying," *Journal of Guidance Control and Dynamics*, vol. 36, no. 1, pp. 185-195, January-February 2015.

[34] H. B. Du and S. H. Li, "Finite-time attitude stabilization for a spacecraft using homogeneous method," *Journal of Guidance Control and Dynamics*, vol. 35, no. 3, pp. 740-748, May-June 2012.

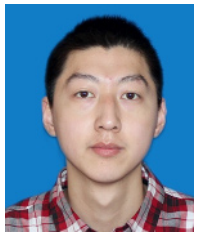

Wei-Shun Sui received his B.S. degree in Electrical Engineering from Northeast Forestry University in 2012. Currently, he is a Ph.D. student in the School of Astronautics at Harbin Institute of Technology. His research interests include spacecraft coordination control, adaptive control, and sliding-mode control.

Guang-Ren Duan received his Ph.D. degree in control systems theory in 1989 from Harbin Institute of Technology, China. From 1989 to 1991, he was a postdoctoral researcher at Harbin Institute of Technology, where he became a professor of control systems theory in 1991. He visited the University of Hull, UK, and the University of Sheffield, UK from December 1996 to October 1998 and worked at the Queen's University of Belfast, UK from October 1998 to October 2002. Since August 2000, he has been elected as specially employed professor at Harbin Institute of Technology sponsored by the Cheung Kong Scholars Program of the Chinese government. He is currently the director of the Center for Control Theory and Guidance Technology at Harbin Institute of Technology. He is a chartered engineer in the UK, a senior member of IEEE and a fellow of IEE. His research interests include robust control, eigenstructure assignment, descriptor systems, missile autopilot design, and spacecraft control.

Ming-Zhe Hou received his B.S. and Ph.D. degrees in Control Science and Engineering from Harbin Institute of Technology, in 2005 and 2011, respectively. Since 2017, he has become an associate professor at Harbin Institute of Technology. His research interests include nonlinear filtering and control, aircraft guidance and control.

Mao-Rui Zhang received his Ph.D. degree in Control Theory and Application from Harbin Institute of Technology, China, 1998. He carried out postdoctoral research at Israel Institute of Technology from 2005 to 2007. He is currently a professor at the School of Astronautics, Harbin Institute of Technology. His main research interests are optimal control, time-delay control and special electro-hydraulic servo system control.